



On and Off Retinal Circuit Assembly by Divergent Molecular Mechanisms

Lu O. Sun *et al.*

Science **342**, (2013);

DOI: 10.1126/science.1241974

This copy is for your personal, non-commercial use only.

If you wish to distribute this article to others, you can order high-quality copies for your colleagues, clients, or customers by [clicking here](#).

Permission to republish or repurpose articles or portions of articles can be obtained by following the guidelines [here](#).

The following resources related to this article are available online at www.sciencemag.org (this information is current as of January 23, 2014):

Updated information and services, including high-resolution figures, can be found in the online version of this article at:

<http://www.sciencemag.org/content/342/6158/1241974.full.html>

Supporting Online Material can be found at:

<http://www.sciencemag.org/content/suppl/2013/10/31/342.6158.1241974.DC1.html>

A list of selected additional articles on the Science Web sites **related to this article** can be found at:

<http://www.sciencemag.org/content/342/6158/1241974.full.html#related>

This article **cites 35 articles**, 7 of which can be accessed free:

<http://www.sciencemag.org/content/342/6158/1241974.full.html#ref-list-1>

This article appears in the following **subject collections**:

Neuroscience

<http://www.sciencemag.org/cgi/collection/neuroscience>

On and Off Retinal Circuit Assembly by Divergent Molecular Mechanisms

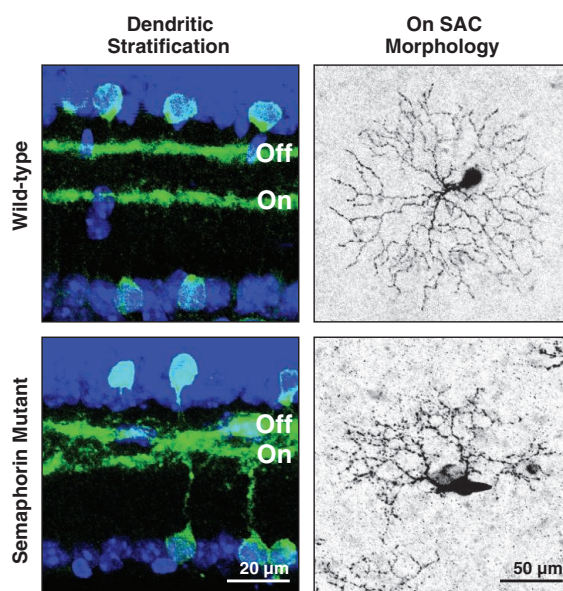
Lu O. Sun, Zheng Jiang, Michal Rivlin-Etzion, Randal Hand, Colleen M. Brady, Ryota L. Matsuoka, King-Wai Yau, Marla B. Feller, Alex L. Kolodkin*

Introduction: Direction-selective responses to visual cues depend upon precise connectivity between inhibitory starburst amacrine cells (SACs) and direction-selective ganglion cells (DSGCs). Motion is detected by SAC responses to illumination onset (On) or cessation (Off). On and Off SACs costratify in the inner plexiform layer of the vertebrate retina with distinct DSGC dendritic arborizations that mediate On or Off directional responses. Here, we study the molecular mechanisms that specify On versus Off SACs and the signaling pathways governing the functional assembly of murine retinal direction-selective circuitry. We show that signaling between the transmembrane guidance cue semaphorin 6A (Sema6A) and its receptor plexinA2 (PlexA2) regulates dendritic morphology of On but not Off SACs, thereby controlling direction-selective responses to visual stimuli.

Methods: We analyzed SAC stratification in the inner plexiform layer, and dendritic morphology of individual On and Off SACs, throughout retinal development in *Sema6A* and *PlexA2* mutant mice. We used dissociated retinal cultures to determine how neurites from genetically labeled SACs respond to exogenous Sema6A. We determined the light-evoked excitatory and inhibitory responses of *Sema6A*^{-/-} On SACs. Finally, we analyzed direction-selective responses in isolated retinas by On-Off direction-selective ganglion cells.

Results: Sema6A is expressed in On, but not Off, SACs, whereas PlexA2 is expressed in all SACs. In vitro, exogenous Sema6A repels neurites only from PlexA2⁺, Sema6A⁻ SACs, the in vivo expression profile of Off SACs. In *PlexA2*^{-/-} or *Sema6A*^{-/-} retinas, SAC dendritic stratifications fail to completely segregate from each other; therefore, in vitro and in vivo observations suggest that repulsive interactions between Sema6A and PlexA2 mediate SAC dendritic stratification. Analysis of dendritic morphology in individual SACs in the *x-y* plane reveals that On SACs in *PlexA2*^{-/-} and *Sema6A*^{-/-} mutants are missing extensive portions of their dendritic fields, have asymmetric dendritic arbors, and exhibit self-avoidance defects; Off SACs in these mutants have normal *x-y* plane dendritic arbors. Specific On-Off bistratified direction-selective ganglion cells in *Sema6A*^{-/-} mutant retinas exhibit decreased tuning of On-directional motion responses, whereas Off responses in these same cells are unaffected, correlating the elaboration of symmetric SAC dendritic morphology and asymmetric responses to motion.

Discussion: Our findings show that, in addition to contributing to the separation between On and Off SAC dendritic stratifications into distinct inner plexiform layer laminae, Sema6A-PlexA2 signaling selectively regulates the elaboration of symmetric On SAC dendritic fields. Disruption of Sema6A-PlexA2 signaling ultimately results in compromised On, but not Off, directional tuning in a subclass of On-Off direction-selective ganglion cells. Our elucidation of molecular events critical for functional assembly of retinal direction-selective circuitry may have general implications for understanding the establishment of circuitry in which individual neurons participate in multiple distinct pathways.



READ THE FULL ARTICLE ONLINE

<http://dx.doi.org/10.1126/science.1241974>



Cite this article as L. O. Sun *et al.*, *Science* 342, 1241974 (2013). DOI: 10.1126/science.1241974

FIGURES IN THE FULL ARTICLE

Fig. 1. Sema6A is expressed in On, but not Off, SACs in vivo, and SACs lacking Sema6A avoid exogenous Sema6A in vitro.

Fig. 2. Sema6A-PlexA2 signaling segregates On and Off SAC dendritic stratifications in vivo.

Fig. 3. Sema6A-PlexA2 signaling regulates dendritic arborization and symmetric organization in On SACs.

Fig. 4. Sema6A-PlexA2 signaling is dispensable for Off SAC dendritic arborization and ChAT⁺ plexus organization.

Fig. 5. On direction-selective tuning of bistratified TRHR-GFP⁺ direction-selective ganglion cells is compromised in *Sema6A*^{-/-} mutants.

Fig. 6. Sema6A-PlexA2 signaling in the development of SACs and the functional assembly of direction-selective retinal circuits.

SUPPLEMENTARY MATERIALS

Materials and Methods

Figs. S1 to S17

Movies S1 to S6

References

Development of direction-selective circuitry. On and Off mouse SACs normally stratify in discrete layers (**top left**) and exhibit radial dendrite morphology (**top right**). Sema6A and its PlexA2 receptor are expressed in On SACs, but only PlexA2 is expressed in Off SACs. In *Sema6A* mutants, SACs fail to stratify (**bottom left**) and On SACs are misshapen (**bottom right**), compromising responses to "light on" directional cues.

The list of author affiliations is available in the full article online.

*Corresponding author. E-mail: kolodkin@jhmi.edu

On and Off Retinal Circuit Assembly by Divergent Molecular Mechanisms

Lu O. Sun,^{1,2} Zheng Jiang,^{1*} Michal Rivlin-Etzion,^{3,*†} Randal Hand,^{1,2} Colleen M. Brady,^{1,2} Ryota L. Matsuoka,^{1,2‡} King-Wai Yau,¹ Marla B. Feller,³ Alex L. Kolodkin^{1,2§}

Direction-selective responses to motion can be to the onset (On) or cessation (Off) of illumination. Here, we show that the transmembrane protein semaphorin 6A and its receptor plexin A2 are critical for achieving radially symmetric arborization of On starburst amacrine cell (SAC) dendrites and normal SAC stratification in the mouse retina. Plexin A2 is expressed in both On and Off SACs; however, semaphorin 6A is expressed in On SACs. Specific On-Off bistratified direction-selective ganglion cells in *semaphorin 6A*^{-/-} mutants exhibit decreased tuning of On directional motion responses. These results correlate the elaboration of symmetric SAC dendritic morphology and asymmetric responses to motion, shedding light on the development of visual pathways that use the same cell types for divergent outputs.

The detection of object motion is a critical visual function. Direction-selective responses to visual cues by the vertebrate retina depend on the precise wiring of inhibitory starburst amacrine cells (SACs) onto direction-selective ganglion cells (DSGCs) (1–4). SACs are divided into onset (On) and cessation (Off) subtypes based on their function, which correlates with localization of their cell bodies and dendritic processes (5). On and Off SACs costratify with distinct DSGC dendritic arborizations that have the capacity to mediate On or Off directional responses (6–8), and SACs play a fundamental role in regulating DSGC output (9–12). Protocadherins mediate the self-avoidance of SAC dendrite processes and regulate the morphogenesis of both On and Off SACs (13). However, the molecular mechanisms that specify On versus Off SACs, and the signaling pathways governing the functional assembly of retinal direction-selective circuitry, remain unclear.

Class A plexin receptors (PlexAs) in the developing mouse retina are expressed largely in the inner plexiform layer (14, 15). To identify cell types expressing PlexA2, we performed double immunohistochemistry analyses and observed colocalization of PlexA2 and choline acetyltransferase (ChAT), which is expressed by SACs (Fig. 1, A to C). This observation was confirmed by *in situ* hybridization analysis (fig. S1, A and C) and by labeling in a *PlexA2-LacZ* reporter mouse (fig. S2, F to I). The protein distributions in the inner

plexiform layer of PlexA2 and semaphorin 6A (Sema6A), a transmembrane semaphorin that is a functional PlexA2 ligand in the mammalian nervous system (16, 17), are complementary with respect to PlexA2 expression in the Off region of the inner plexiform layer, but they exhibit selective overlap in the On region of the inner plexiform layer (Fig. 1, D to F, and fig. S1, E to H'). Sema6A immunoreactivity accumulates along the inner of the two PlexA2-immunopositive (PlexA2⁺) sublaminae, is observed in On but not Off inner plexiform layer neurites, and is found in the cell bodies of all PlexA2⁺ cells in the ganglion cell layer but not the inner nuclear layer (Fig. 1, G to I). Thus, Sema6A and PlexA2 are coexpressed in On, but not Off, SACs.

To investigate the functional importance of this selective PlexA2 and Sema6A protein localization, we isolated SACs from a mouse line, *ChAT::cre;ROSA^{LSL-TdTomato}*, in which both On and Off SACs are genetically labeled with TdTomato (fig. S3, A to C), and cultured them *in vitro* on stripes coated with recombinant Sema6A-Fc protein. As we observed *in vivo*, there are two populations of SACs in culture: Sema6A-positive (Sema6A⁺) and Sema6A⁻ SACs (fig. S1, I to K'). Neurites from wild-type Sema6A⁻ SACs avoid Sema6A-Fc stripes, whereas wild-type Sema6A⁺ SACs show no preference and extend their processes freely over Sema6A-Fc and control stripes (Fig. 1, J to K' and N). In contrast, both Sema6A⁻ and Sema6A⁺ SACs derived from *PlexA2*^{-/-} mutant retinas extend neurites equally over Sema6A-Fc and control stripes (Fig. 1, L to N), showing that *in vitro* exogenous Sema6A repels processes only from SACs that express PlexA2 but not Sema6A—the expression profile of Off SACs *in vivo*.

To address PlexA2 function in retinal development *in vivo*, we first characterized SAC sublaminae neurite stratification and SAC cell body mosaic patterning in *PlexA2*^{-/-} retinas. SACs normally stratify in two discrete inner plexiform layer laminae: S2 and S4 (Fig. 2A). In *PlexA2*^{-/-} retinas,

however, these two stratifications fail, with full penetrance, to completely segregate from each other (Fig. 2B, and fig. S4, A and A'; *n* = 6 *PlexA2*^{-/-} mutants). This is in contrast to calretinin⁺ amacrine cells and retinal ganglion cells, TH⁺ and vGlut3⁺ amacrine cells, and NK3R⁺, Syt2⁺, and PKCα⁺ bipolar cells, all of which show normal axonal targeting and dendritic stratifications in the *PlexA2*^{-/-} retina (fig. S4, B to G'). In addition, *PlexA2*^{-/-} On and Off SACs exhibit indistinguishable density recovery profiles, and several additional cell body mosaic spacing parameters, compared with control SACs (fig. S5), showing that PlexA2 is dispensable for regulating SAC cell body mosaic spacing.

The *in vivo* protein distribution of PlexA2 and Sema6A in the inner plexiform layer, and the responses to Sema6A protein by SAC neurites *in vitro* (Fig. 1), suggest that Sema6A is involved in PlexA2-dependent SAC dendritic stratification. We tested this idea by analyzing *Sema6A*^{-/-} mutant retinas and found that *PlexA2*^{-/-} SAC dendritic stratification defect is phenocopied, with full penetrance and expressivity, in *Sema6A*^{-/-} retinas (Fig. 2C; *n* = 6 *Sema6A*^{-/-} mutants) and is not further enhanced in *PlexA2*^{-/-}; *Sema6A*^{-/-} double mutant retinas (*dKO*) (Fig. 2, D and H; *n* = 4 *PlexA2*^{-/-}; *Sema6A*^{-/-} mutants). This suggests that *PlexA2* and *Sema6A* are involved in the same signaling pathway that regulates SAC dendritic stratification in the inner plexiform layer (Fig. 2G). To determine whether the segregation of On and Off SAC processes is cell-type-autonomous, we generated a *ChAT::cre;PlexA2^{fl/fl}* mouse line in which PlexA2 is selectively ablated in all SACs (fig. S2, J to M). We observed in these mutant retinas the same stratification defects we found in *PlexA2*^{-/-} mice (Fig. 2, E, F, and H, and fig. S2, J' to M'). SAC dendritic stratification defects were not observed in other *PlexA* null mutant mice (*PlexA1*^{-/-}, *PlexA3*^{-/-}, and *PlexA4*^{-/-}) (fig. S6, A to C) or *neuropilin-1* and -2 deficient mice (fig. S6, D to F), suggesting that most secreted semaphorins do not mediate SAC stratification. The same is true for mutants in the genes encoding the remaining class 6 semaphorin proteins (*Sema6B*, *6C*, and *6D*) (18).

In early postnatal development, wild-type On and Off SAC processes are initially entangled at P0 and P2 but segregate into two distinct stratifications by P4 (Fig. 2I to K') (6, 19). We found that On and Off SAC dendrites in *ChAT::cre;ROSA^{LSL-TdTomato} PlexA2*^{-/-} mice failed to completely segregate by P4 (Fig. 2, O and O'). To further investigate these SAC dendritic process stratification defects, in which On and Off SAC processes apparently cross over between inner plexiform layers 2 and 4, we analyzed sparsely labeled SACs in *ChAT::cre^{ER};ROSA^{LSL-TdTomato}; PlexA2*^{-/-} mutant retinas. We observed that dendrites of both On and Off SACs stratify normally in control retinas (*PlexA2*^{+/+}) but that both SAC types can stratify inappropriately in the

¹Solomon H. Snyder Department of Neuroscience, The Johns Hopkins University School of Medicine, Baltimore, MD 21205, USA. ²Howard Hughes Medical Institute, Baltimore, MD 21205, USA. ³Department of Molecular and Cell Biology and the Helen Wills Neuroscience Institute, University of California, Berkeley, Berkeley, CA 94720, USA.

*These authors contributed equally to this work

†Present address: Department of Neurobiology, Weizmann Institute of Science, Rehovot 76100, Israel.

‡Present address: Department of Developmental Genetics, Max Planck Institute for Heart and Lung Research, 61231 Bad Nauheim, Germany.

§Corresponding author. E-mail: kolodkin@jhmi.edu

PlexA2^{-/-} mutants (fig. S3). We examined 35 *PlexA2*^{-/-} SAC processes that crossed between the On and Off ChAT bands and traced 17 of these to Off SACs and 18 to On SACs (fig. S3, D to L). Therefore, both in vitro and in vivo observations support the idea that *Sema6A*-*PlexA2* repulsive interactions are a critical component of the mo-

lecular mechanisms that underlie stratification of On and Off SAC dendritic processes.

The formation of distinct On and Off SAC sublamina dendritic process stratifications during early retinal development differentiates these two motion-detection circuits. Because *Sema6A* is expressed selectively and continuously in On,

but not Off, SACs (Fig. 1 and fig. S1), we next asked if *Sema6A*-*PlexA2* signaling functions later in retinal development to refine direction-selective circuitry by regulating On SAC dendritic morphology. To visualize On SAC dendritic morphology, we filled individual adult On SACs with Alexa-555 dye and confirmed their identity by

Fig. 1. *Sema6A* is expressed in On, but not Off, SACs in vivo, and SACs lacking *Sema6A* avoid exogenous *Sema6A* in vitro. (A to C)

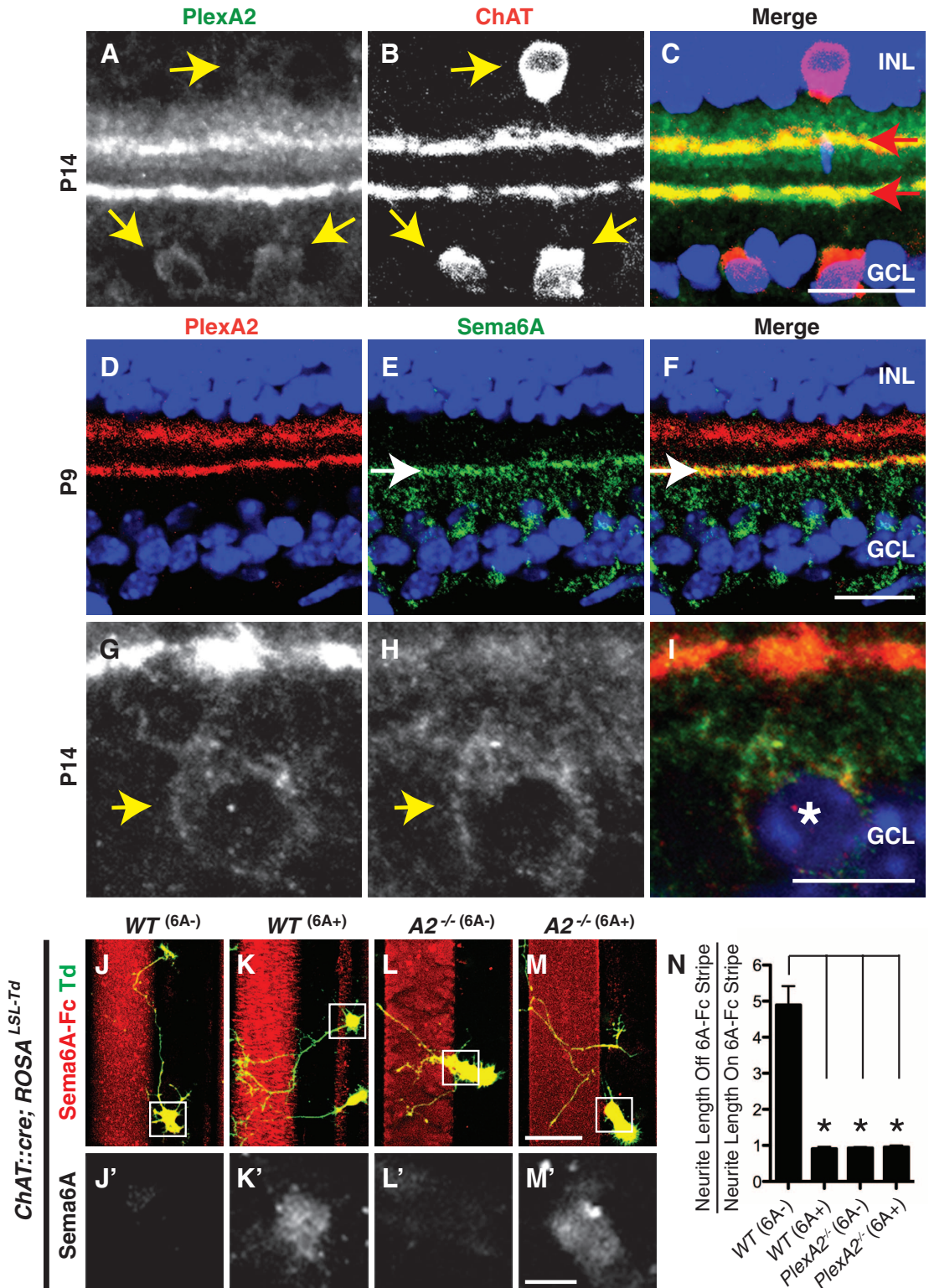
Mouse P14 retina sections immunostained with antibodies directed against *PlexA2* (green) and ChAT (red) reveal colocalization of *PlexA2* and ChAT immunoreactivity in cell bodies (yellow arrows) and in dendritic processes (red arrows).

(D to I) Postnatal retina sections immunostained with antibodies to *PlexA2* (red) and antibodies to *Sema6A* (green) show that *PlexA2* and *Sema6A* exhibit mostly complementary protein distributions in the inner plexiform layer [white arrows in (E) and (F)] but that they are coexpressed in On SACs [yellow arrow heads in (G) and (H), white asterisk in (I)].

(J to N) Genetically labeled, dissociated SACs from wild-type (WT) retinas are divided into two populations in vitro: *Sema6A*⁻ (J and J') and *Sema6A*⁺ (K and K'). Neurites extending from WT *Sema6A*⁻ SACs avoid exogenous *Sema6A*-Fc stripes (J), whereas WT *Sema6A*⁺ SACs do not (K).

PlexA2^{-/-} SACs, both *Sema6A*⁺ and *Sema6A*⁻, extend freely over *Sema6A*-Fc stripes [(L) and (M)]. The ratio of SAC neurite length off of *Sema6A*-Fc stripes to neurite length on *Sema6A*-Fc stripes is shown in (N) ($n \geq 15$ SACs per genotype). Error bars, mean \pm SEM. * $P < 0.01$.

Scale bars, 20 μ m in (C) for (A) to (C), 20 μ m in (F) for (D) to (F), 10 μ m in (I) for (G) to (I), 40 μ m in (M) for (J) to (M), and 10 μ m in (M') for (J') to (M').



anti-ChAT immunostaining (fig. S7, A to C). Wild-type On SACs exhibited characteristic radially symmetric morphology (Fig. 3A), whereas *PlexA2*^{-/-} On SACs were missing extensive portions of their dendritic fields (Fig. 3B). Also,

normal SAC dendritic self-avoidance was compromised in *PlexA2*^{-/-} On SACs (Fig. 3, A' and B', and fig. S7, D to G). Unlike SAC self-avoidance defects previously described in protocadherin mutants (13), the *PlexA2*^{-/-} defects were con-

fined to the distal-most third of SAC dendritic processes. These same defects were found in *Sema6A*^{-/-} and *PlexA2*^{-/-}; *Sema6A*^{-/-} mutants (Fig. 3, C to D'). Quantification of total dendritic length (Fig. 3E), dendritic field area (Fig. 3F),

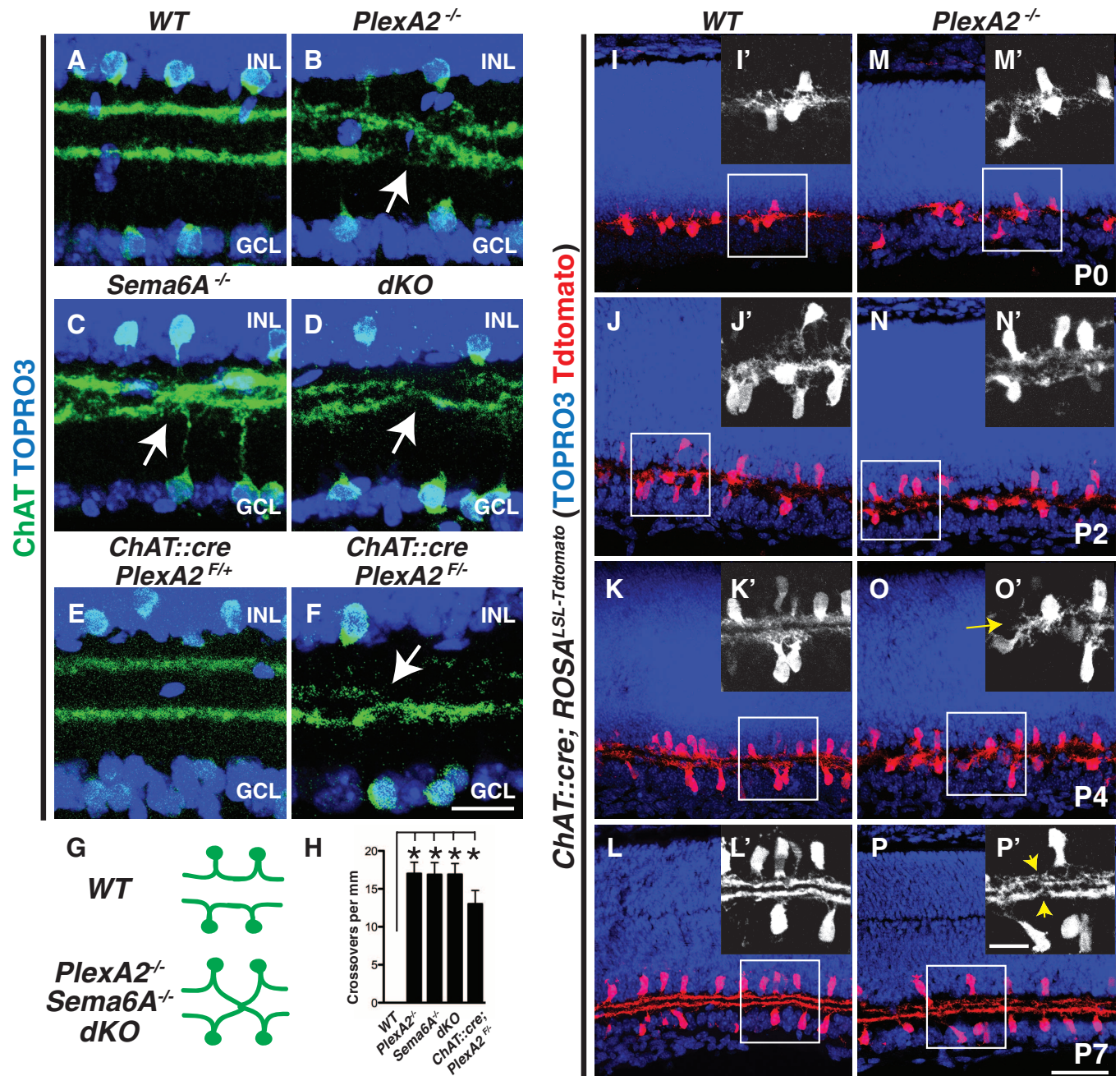


Fig. 2. *Sema6A*-*PlexA2* signaling segregates On and Off SAC dendritic stratifications in vivo. (A to D) Wild-type (A), *PlexA2*^{-/-} (B), *Sema6A*^{-/-} (C), and *PlexA2*^{-/-}; *Sema6A*^{-/-} (D) adult retina sections immunostained with antibodies to ChAT. On and Off SAC processes fail, with full penetrance, to completely segregate in *PlexA2*^{-/-} (B), *Sema6A*^{-/-} (C), and *PlexA2*^{-/-}; *Sema6A*^{-/-} (D) retinas (stratification crossovers indicated by white arrows, $n \geq 4$ mice for each genotype). (E and F) Conditional removal of *PlexA2* protein in SACs recapitulates *PlexA2*^{-/-} stratification defects ($n = 3$ mice). (G) Schematics of SAC dendritic stratification in WT, *PlexA2*^{-/-}, *Sema6A*^{-/-}, and *PlexA2*^{-/-}; *Sema6A*^{-/-} mutants. (H) Quantification of SAC stratification crossovers in (A) to (D) and in (F) ($n \geq 6$ retinas per genotype). Error bars, mean \pm SD * $P <$

0.001. (I to P') Characterization of SAC dendritic stratification in WT [(I) to (L')] and *PlexA2*^{-/-} [(M) to (P')] retinas using the SAC Tdtomato genetic reporter. In WT retinas, On and Off SAC dendrites are intermingled at P0 [(I) and (I')]. They then segregate during early postnatal retinal development [(J) and (J')] and become completely separate stratifications by P4 [(K) and (K')]. SAC dendritic stratifications in *PlexA2*^{-/-} mutants [(M), (M'), (N), and (N')] are indistinguishable from WT [(I), (I'), (J), and (J')] at P0 and at P2. However, the stratification phenotype is observed by P4 in *PlexA2*^{-/-} retinas [(O) and (O')], yellow arrow) and persists through P7 [(P) and (P')], yellow arrowheads). $n = 3$ mice for each genotype at each different developmental stage. Scale bars, 20 μ m in (F) for (A) to (F), 50 μ m in (P) for (I) to (P), and 20 μ m in (P') for (I') to (P').

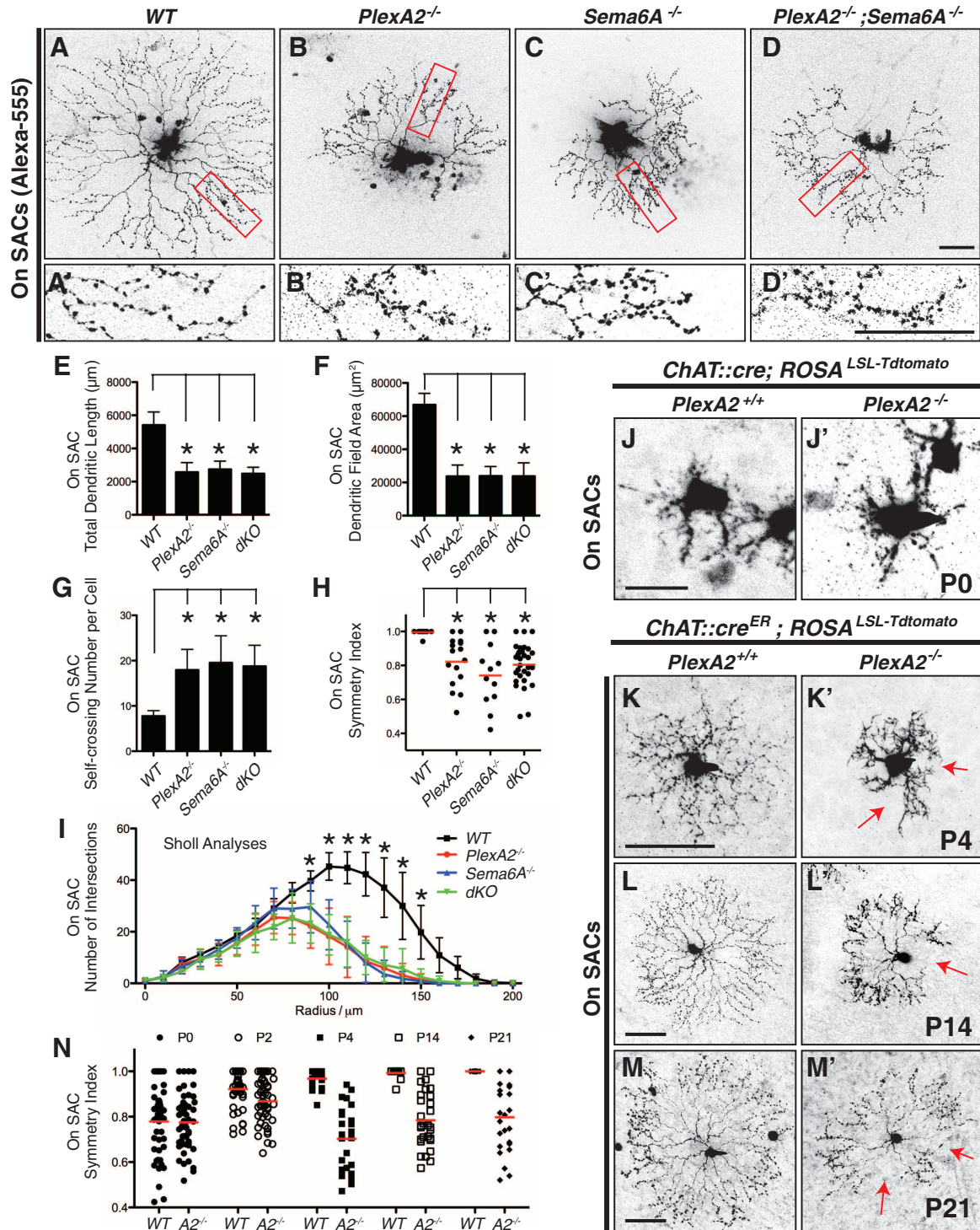


Fig. 3. Sema6A-PlexA2 signaling regulates dendritic arborization and symmetric organization in On SACs. (A to D) Single On SACs labeled with Alexa-555 in WT (A), *PlexA2*^{-/-} (B), *Sema6A*^{-/-} (C), and *PlexA2*^{-/-};*Sema6A*^{-/-} (D) adult retinas. (A' to D') Single-plane confocal images of magnified fields in (A) to (D) (red rectangles) show that higher-order distal dendrites in *PlexA2*^{-/-} (B'), *Sema6A*^{-/-} (C'), and *PlexA2*^{-/-};*Sema6A*^{-/-} (D') retinas exhibit self-avoidance defects in comparison with WT (A'). (E to I) Quantification of total dendritic length (E), dendritic field area (F), self-crossing number per cell (G), symmetry index (H), and dendritic complexity (I, measured by Sholl analyses) shows that overall dendritic morphology is disrupted in *PlexA2*^{-/-}, *Sema6A*^{-/-}, and *PlexA2*^{-/-};*Sema6A*^{-/-} retinas ($n \geq 12$ SACs per genotype). Error bars, mean \pm SD.

* $P < 0.01$. (J to M') Sparse genetic labeling of On SACs in WT retinas [(J) to (M)] shows that dendritic morphology of On SACs is not symmetric at P0 (J) but becomes symmetric during the course of early postnatal retinal development [(K) to (M)]. *PlexA2*^{-/-} On SACs (J') are indistinguishable from WT (J) at P0; however, they fail to establish dendritic process symmetry by P4 [red arrows in (K')] and throughout retinal development [red arrows in (L') and (M')]. (N) Quantification of the symmetry index in WT and *PlexA2*^{-/-} retinas through early postnatal retinal development. Red bars in (H) and (N) represent the mean value for each genotype. Scale bars, 50 μ m in (D) for (A) to (D), 50 μ m in (D') for (A') to (D'), 20 μ m in (J) for (J) and (J'), 50 μ m in (K) for (K) and (K'), 50 μ m in (L) for (L) and (L'), and 50 μ m in (M) for (M) and (M').

self-crossing number per SAC (Fig. 3G), symmetry index (Fig. 3H; defined in fig. S7I), and dendritic complexity (Sholl analysis, Fig. 3I) reveals that the overall dendritic arborization characteristics and symmetric dendritic organization are compromised in *PlexA2*^{-/-}, *Sema6A*^{-/-}, and *PlexA2*^{-/-}; *Sema6A*^{-/-} mutants.

In the developing rabbit retina, On SAC dendritic processes achieve symmetry by postnatal day 0 (P0) (20). In addition to our Alexa-555 injection experiments in adult mice, we used genetic sparse labeling to delineate On SAC morphology throughout postnatal murine retinal development. Wild-type On SACs exhibit asymmetric dendritic morphology at P0 and P2 (Fig. 3J and fig. S8A, top left panels) and display extensive dendritic

process motility early postnatally (movie S1). As early as P4, however, symmetric radial dendritic process organization was achieved (Fig. 3K and fig. S8A, bottom left panels) and then maintained throughout retinal development (Fig. 3, L to N). At P0, *PlexA2*^{-/-} On SAC dendrites resemble wild-type with respect to dendritic asymmetry and other dendritic organization parameters (Fig. 3, J' and N, $P = 0.9884$; and fig. S8, A and B); they also exhibit similar dendritic process motility (movie S2). Nonetheless, they still retain asymmetric dendritic morphology at P4 (Fig. 3, K' and N, $P < 0.001$; and fig. S8A, bottom right panels) or even later (P14 and P21) (Fig. 3, L', M', and N, $P < 0.001$; and fig. S8C). These same defects apply to *Sema6A*^{-/-} mutant retinas (fig. S9). We

did not observe any correlation between SAC dendritic asymmetry phenotypes and the overall location of On SAC cell bodies in *PlexA2*^{-/-} retinas; *PlexA2*^{-/-} On SACs in all four retinal quadrants exhibit the full range of dendritic process symmetry defects (fig. S10). Thus, in addition to contributing to the separation between On and Off SAC dendritic stratifications into distinct inner plexiform layer laminae, *Sema6A*-*PlexA2* signaling regulates the elaboration of symmetric On SAC dendritic fields during postnatal retina development.

To investigate whether *PlexA2*^{-/-} On SAC inner plexiform layer dendritic arborization phenotypes in the *x-y* plane (Fig. 3) are correlated with SAC dendritic stratification defects in the *z* plane

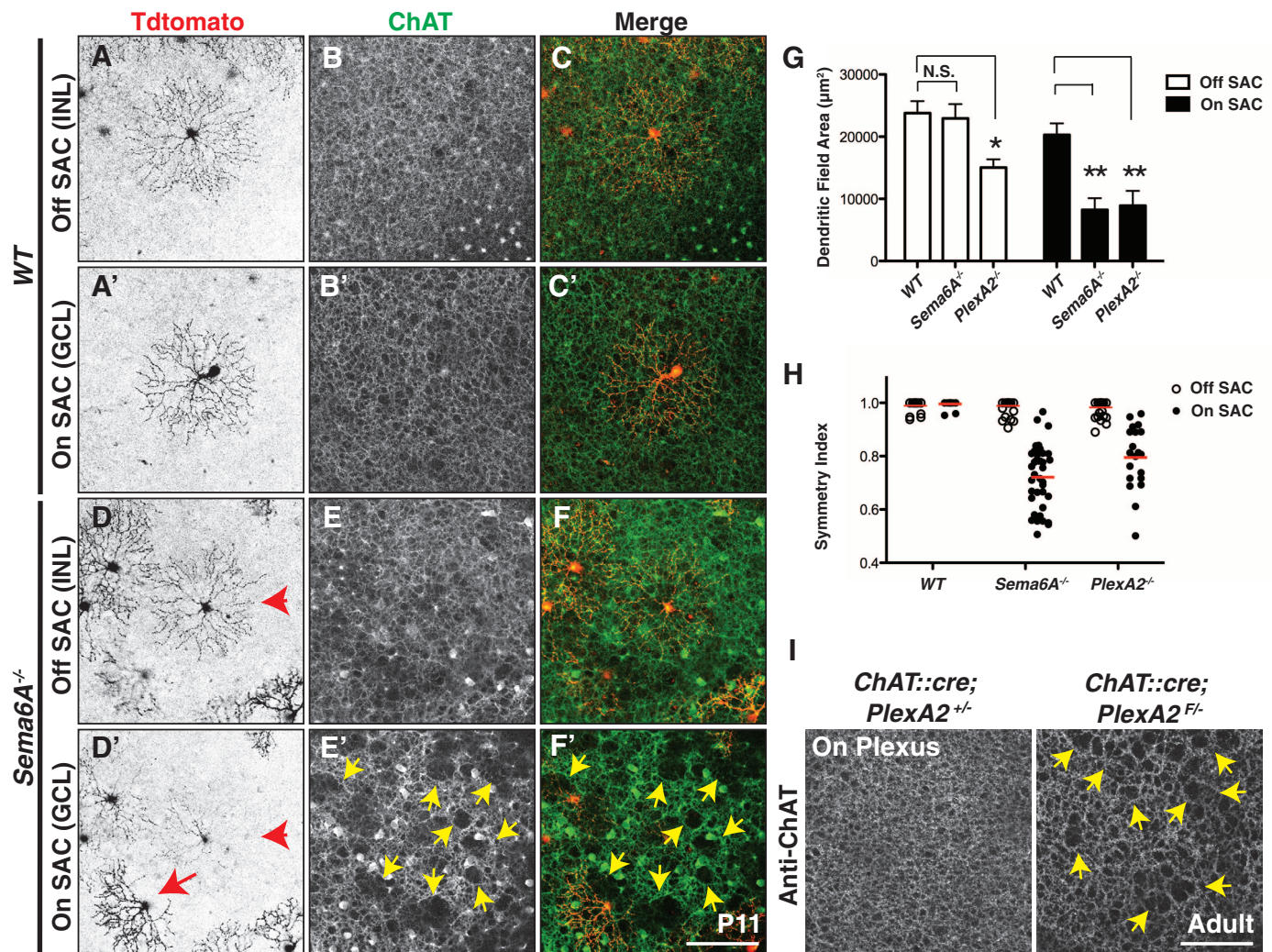


Fig. 4. *Sema6A*-*PlexA2* signaling is dispensable for Off SAC dendritic arborization and *ChAT*⁺ plexus organization. (A to F') Sparse genetic labeling of On [(A') and (D')] and Off [(A) and (D)] SACs coupled with anti-*ChAT* immunostaining of On [(B') and (E')] and Off [(B) and (E)] SAC dendritic plexuses in the same WT [(A) to (C')] and *Sema6A*^{-/-} [(D) to (F')] retinas. (D) to (F) and (D') to (F') are different focal planes from the same field. On and Off SACs in WT retinas exhibit stereotypic symmetrical morphology [(A) and (A')]. In contrast, overall dendritic organization of *Sema6A*^{-/-} On SACs [(D)], red arrow, but not Off SACs [(D) and (D')], red arrowhead, is disrupted. Similarly, SAC plexus organization revealed by anti-*ChAT* immunostaining

shows that only the *Sema6A*^{-/-} On SAC plexus is compromised, as indicated by large gaps and holes [yellow arrowheads in (E') and (F')]. (G and H) Quantification of dendritic field area (G) and symmetry index (H) of WT, *Sema6A*^{-/-}, and *PlexA2*^{-/-} On and Off SACs at P11. Red bars in (H) represent mean value for each genotype. Error bars, mean \pm SD. * $P < 0.01$; ** $P < 0.001$. (I) Dendritic plexus organization of On SACs in control (left) and *ChAT::cre*;*PlexA2*^{F/-} (right) retinas. Conditional removal of *PlexA2* protein in all SACs disrupts On, but not Off (see fig. S14, A and B), SAC plexus (yellow arrowheads in right panel). Scale bars, 100 μ m in (F') for (A) to (F'), 100 μ m in (I) for left and right panels.

of the inner plexiform layer (Fig. 2, A to D), we analyzed both the x - y projection images and z -stacked images of individual, genetically labeled, *PlexA2*^{-/-} On SACs. We found two classes of *PlexA2*^{-/-} On SACs: (i) those that stratify normally within the ChAT⁺ On sublaminae (11 out of 29 On SACs) (fig. S11, B and B'), and (ii) those that misstratify within the ChAT⁺ Off sublaminae (18 out of 29 On SACs) (fig. S11, C and C'). However, whether these *PlexA2*^{-/-} mutant SACs exhibit normal or aberrant dendritic stratification

within the ChAT⁺ sublaminae, they show the same dendritic field symmetry defects (fig. S11, D to G, and movie S3). Thus, *PlexA2*^{-/-} On SAC dendritic arborization phenotypes in the x - y plane are distinct from SAC dendritic stratification defects in the z plane.

The restricted expression of *Sema6A* in On SACs raises the possibility that *Sema6A* regulates only On, but not Off, SAC dendritic arborization in the x - y plane. In contrast, protocadherins expressed in both On and Off SACs (27) dictate

dendritic self-avoidance in both cell types (13). We investigated this issue by examining genetically labeled Off SACs. Indeed, *Sema6A*^{-/-} Off SACs (Fig. 4D) exhibit the normal, radially symmetric, dendritic morphology found in wild-type SACs (Fig. 4, A and A', quantified in Fig. 4H, and movie S4). *Sema6A*^{-/-} Off SACs also have normal dendritic field area, but *Sema6A*^{-/-} On SACs are abnormal (Fig. 4, D' and G). *PlexA2*^{-/-} Off SACs (figs. S12 and S13 and Fig. 4H) exhibit symmetric dendritic fields, both within and

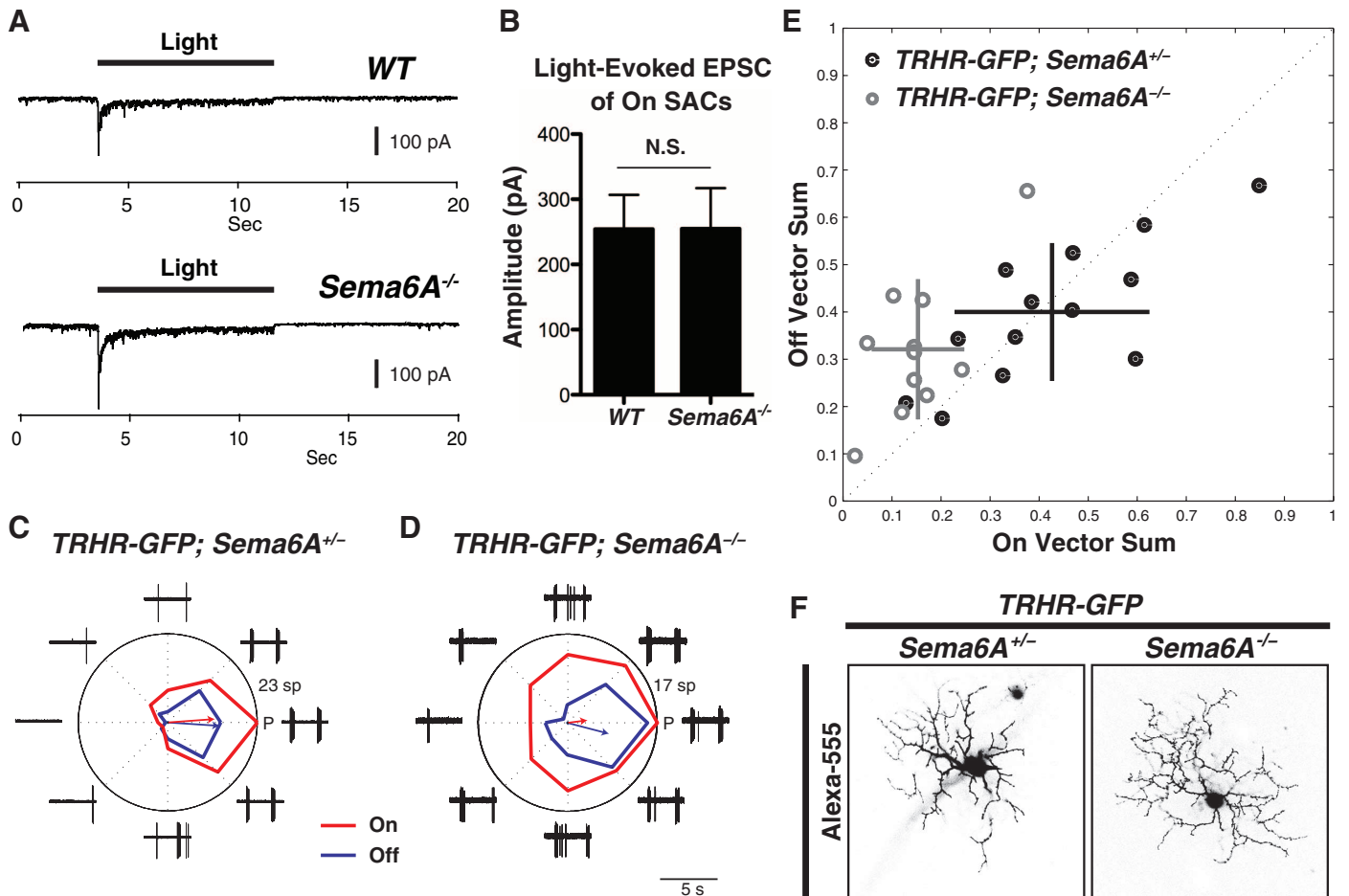


Fig. 5. On direction-selective tuning of bistratified *TRHR-GFP*⁺ direction-selective ganglion cells is compromised in *Sema6A*^{-/-} mutants. (A) Representative light-evoked EPSC traces of WT (top) and *Sema6A*^{-/-} (bottom) On SACs (voltage-clamped at -70mV for both). Recordings from WT ($n = 7$) and *Sema6A*^{-/-} ($n = 8$) On SACs show similar excitatory light responses. (B) The amplitude of light-evoked EPSCs is the same in WT and *Sema6A*^{-/-} On SACs. Error bars, mean \pm SEM. (C and D) Responses by *TRHR-GFP*⁺ On-Off direction-selective ganglion cells to drifting bars from individual *TRHR-GFP*; *Sema6A*^{+/-} RGCs (C) and *TRHR-GFP*; *Sema6A*^{-/-} RGCs (D). The red tuning curve shows the mean On response (spike count during On response phase), and the blue tuning shows the mean Off response (spike count during Off response phase); red and blue arrows indicate vector sums of the On and Off responses, respectively. Traces show the response data for one repetition of bar stimuli (5 s for each trial). P, posterior direction in visual coordinates; sp, total number of spikes. (E) On vector sum values versus Off vector sum values for *TRHR-GFP*; *Sema6A*^{+/-} cells (black filled circles) and *TRHR-GFP*; *Sema6A*^{-/-} cells (gray rings). Horizontal and vertical lines represent SD values. (F) Alexa-555 dye-fills of individual *TRHR-GFP*⁺ On-Off direction-selective ganglion cells and immunostaining with antibody to VACHT in P30 *Sema6A*^{+/-} (left column) and *Sema6A*^{-/-} mutants (right column) reveal that *TRHR-GFP*; *Sema6A*^{-/-} On-Off direction-selective ganglion cells still cofasciculate with On SAC dendritic processes and display normal dendritic arbor morphology in the On plexus (also see fig. S16). Scale bars, 100 μ m in the middle right panel of (F) for top and middle panels, 25 μ m in the bottom right panel of (F) for the bottom two panels.

outside of regions where On and Off SAC dendrites fail to separate from one another (fig. S11H). Reconstruction of individual *PlexA2*^{+/+} and *PlexA2*^{-/-} Off SAC dendritic arbors further illustrates that a fraction of mutant Off SAC dendritic processes from an individual SAC can stratify within the ChAT⁺ On sublamina without affecting the symmetric morphology of the entire Off SAC dendritic arbor (movies S5 and S6). We observed that *PlexA2*^{-/-} On SACs show a modest reduction in dendritic field area (Fig. 4G and fig. S13H), suggesting that PlexA2 may promote dendritic-process outgrowth in Off SACs.

The dendritic arborization defects observed in individual *Sema6A*^{-/-} and *PlexA2*^{-/-} mutant SACs can be generalized to the overall On SAC dendritic plexus organization. Using anti-ChAT immunostaining to label all On and Off SAC

dendritic processes, we observed that only On SAC dendritic plexuses are defective in *Sema6A*^{-/-} retinas (compare Fig. 4E' with Fig. 4, B, B', and E; quantification in fig. S12G). Large gaps and holes in the ChAT⁺ plexuses were found in areas where *Sema6A*^{-/-} On SACs failed to elaborate their dendrites (compare Fig. 4F' with Fig. 4, C, C', and F). The organization of the On SAC dendritic plexus is not likely mediated by the other Sema6 proteins because *Sema6B*^{-/-} and *Sema6C*^{-/-}; *Sema6D*^{-/-} double mutants exhibit normal On and Off SAC plexus organization (fig. S14C; quantification in fig. S14D). Defects in the *PlexA2*^{-/-} ChAT⁺ On plexus phenocopy those observed in *Sema6A*^{-/-} mutants (fig. S12, B to F'; quantification in S12G), and conditional removal of *PlexA2* in all SACs disrupts On, but not Off, ChAT⁺ dendritic plexus organization (Fig. 4I

and fig. S14, A and B). These results show that PlexA2 is cell-type-autonomously required for On, but not Off, SAC plexus organization.

To investigate the correlation between SAC morphological defects and function (22), we performed patch-clamp recordings from labeled On SACs in flat-mount retinas of *ChAT::cre; ROSA^{LSL-TdTomato}* mice in wild-type or *Sema6A*^{-/-} genetic backgrounds. Although *Sema6A*^{-/-} On SACs exhibit reduced dendritic length, coverage area, complexity, and symmetric organization (Fig. 3), the average amplitude of the light-evoked excitatory postsynaptic current (EPSC) is not different from wild-type (Fig. 5, A and B), showing that *Sema6A*^{-/-} On SACs retain normal light-evoked excitatory responses. However, *Sema6A*^{-/-} On SACs showed excess and aberrant light-evoked inhibitory postsynaptic currents (IPSCs) (fig. S15, A to C)

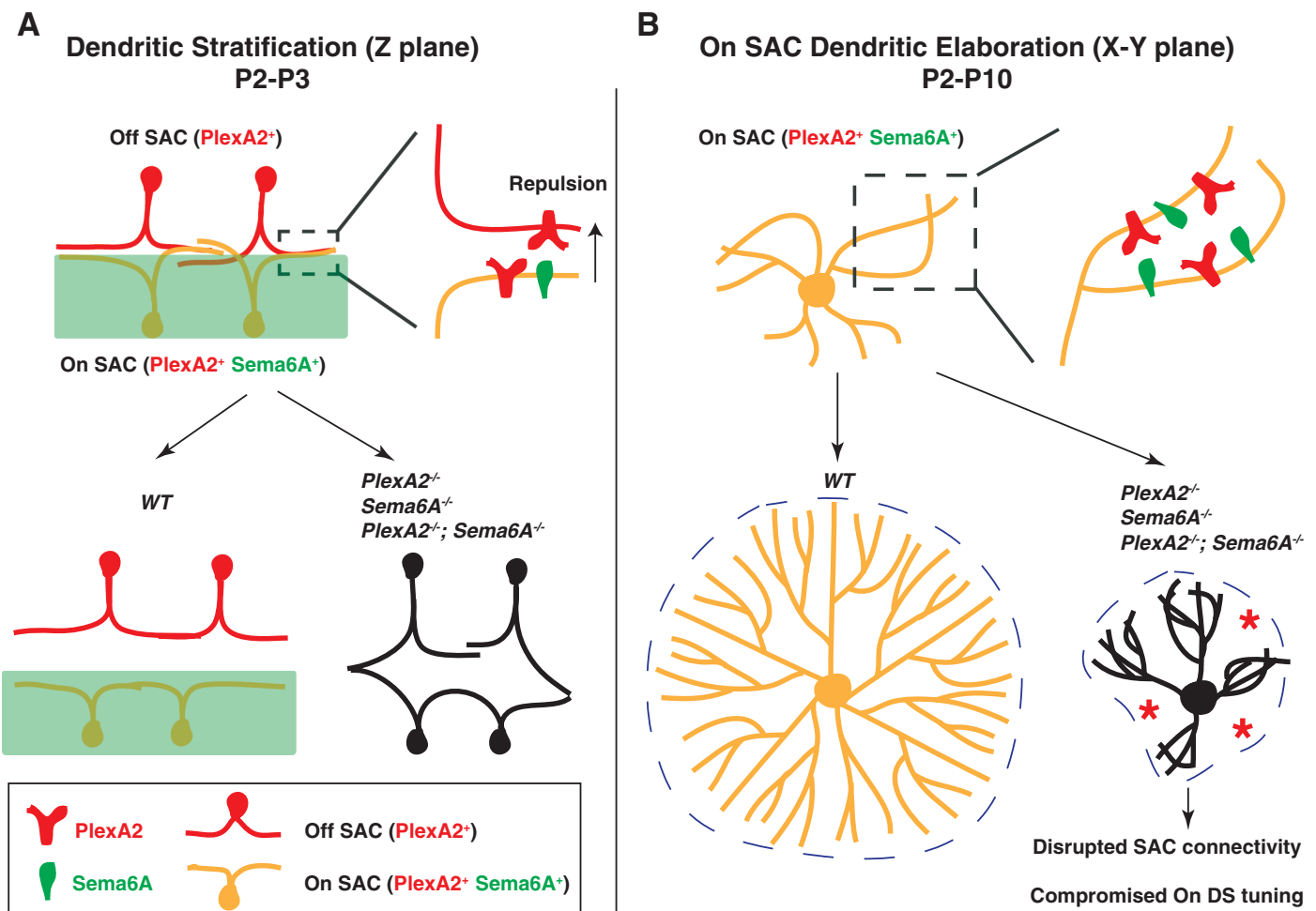


Fig. 6. Sema6A-PlexA2 signaling in the development of SACs and the functional assembly of direction-selective retinal circuits. Sema6A-PlexA2 signaling participates in two aspects of SAC development in the early postnatal mammalian retina. (A) In the z plane, PlexA2 is expressed in both On and Off SACs, whereas Sema6A is expressed only in the lower half of the inner plexiform layer and in On, but not Off, SACs. Repulsive Sema6A-PlexA2 signaling in trans segregates initially entangled On and Off SAC processes between P2 and P3. (B) In the x-y plane, continuous expression of both Sema6A and PlexA2 in On SACs functions to separate rapidly extending dendritic processes throughout early retinal development (P2 to P10). In WT

retinas, On SACs are not symmetrically organized at P0. In the presence of intact Sema6A and PlexA2 signaling, On SAC dendrites avoid each other during this early phase of SAC dendritic development, leading to elaboration of symmetric SAC dendritic fields by the end of postnatal retinal development. In the absence of Sema6A, PlexA2, or both, many On SAC dendrites fail to fully separate from one another. This affects dendritic process dynamics and eventually causes dendritic field area and symmetry defects in *Sema6A*^{-/-}, *PlexA2*^{-/-}, and *Sema6A*^{-/-}; *PlexA2*^{-/-} mutants. The disruption of On SAC dendritic plexuses affects GABA-mediated connectivity among On SACs and compromises directional tuning of On direction-selective responses.

18. R. L. Matsuoka, L. O. Sun, K. Katayama, Y. Yoshida, A. L. Kolodkin, *Sema6B*, *Sema6C*, and *Sema6D* expression and function during mammalian retinal development. *PLoS ONE* **8**, e63207 (2013). doi: [10.1371/journal.pone.0063207](https://doi.org/10.1371/journal.pone.0063207); pmid: [23646199](https://pubmed.ncbi.nlm.nih.gov/23646199/)
19. K. J. Ford, M. B. Feller, Assembly and disassembly of a retinal cholinergic network. *Vis. Neurosci.* **29**, 61–71 (2012). doi: [10.1017/S0952523811000216](https://doi.org/10.1017/S0952523811000216); pmid: [21787461](https://pubmed.ncbi.nlm.nih.gov/21787461/)
20. R. O. Wong, S. P. Collin, Dendritic maturation of displaced putative cholinergic amacrine cells in the rabbit retina. *J. Comp. Neurol.* **287**, 164–178 (1989). doi: [10.1002/cne.902870203](https://doi.org/10.1002/cne.902870203); pmid: [2477402](https://pubmed.ncbi.nlm.nih.gov/2477402/)
21. J. L. Lefebvre, Y. Zhang, M. Meister, X. Wang, J. R. Sanes, Gamma-Protocadherins regulate neuronal survival but are dispensable for circuit formation in retina. *Development* **135**, 4141–4151 (2008). doi: [10.1242/dev.027912](https://doi.org/10.1242/dev.027912); pmid: [19029044](https://pubmed.ncbi.nlm.nih.gov/19029044/)
22. B. N. Peters, R. H. Masland, Responses to light of starburst amacrine cells. *J. Neurophysiol.* **75**, 469–480 (1996). pmid: [8822571](https://pubmed.ncbi.nlm.nih.gov/8822571/)
23. K. Yoshida *et al.*, A key role of starburst amacrine cells in originating retinal directional selectivity and optokinetic eye movement. *Neuron* **30**, 771–780 (2001). doi: [10.1016/S0896-6273\(01\)00316-6](https://doi.org/10.1016/S0896-6273(01)00316-6); pmid: [11430810](https://pubmed.ncbi.nlm.nih.gov/11430810/)
24. M. Rivlin-Etzion *et al.*, Transgenic mice reveal unexpected diversity of on-off direction-selective retinal ganglion cell subtypes and brain structures involved in motion processing. *J. Neurosci.* **31**, 8760–8769 (2011). doi: [10.1523/JNEUROSCI.0564-11.2011](https://doi.org/10.1523/JNEUROSCI.0564-11.2011); pmid: [21677160](https://pubmed.ncbi.nlm.nih.gov/21677160/)
25. L. Haklai-Topper, G. Mlechkovich, D. Savariego, I. Gokhman, A. Yaron, Cis interaction between Semaphorin6A and Plexin-A4 modulates the repulsive response to Sema6A. *EMBO J.* **29**, 2635–2645 (2010). doi: [10.1038/emboj.2010.147](https://doi.org/10.1038/emboj.2010.147); pmid: [20606624](https://pubmed.ncbi.nlm.nih.gov/20606624/)

Acknowledgments: We thank D. Ginty for the *ROSA^{LSL-TdTomato}* mice, J. Nathans for *Six3-cre*, *CHAT::cre*, *CHAT::cre^{ER}*, and *ROSA^{iAP}* mice, and Y. Yoshida for the *Sema6B^{-/-}* and *Sema6C^{-/-};6D^{-/-}* eyes. We also thank S. Hattar, M. Riccomagno,

and Q. Wang for comments on the manuscript and all Kolodkin laboratory members for assistance and discussions throughout the course of this project. This work was supported by NS35165 (A.L.K.); EY06837 (K.-W.Y.); EY019498 and EY013528 (M.B.F.); and the Human Frontier Science Program Organization, the National Postdoctoral Award Program for Advancing Women in Science, and the Edmond and Lily Safra (ELSC) Fellowship for postdoctoral training in Brain Science (M.R.-E.). A.L.K. is an investigator of the Howard Hughes Medical Institute.

Supplementary Materials

www.sciencemag.org/content/342/6158/1241974/suppl/DC1
Materials and Methods
Figs. S1 to S17
Movies S1 to S6
References (26–35)

17 June 2013; accepted 25 September 2013
[10.1126/science.1241974](https://doi.org/10.1126/science.1241974)